

Transverse Momentum Dependence of Electron and Hole Tunneling in a Full Band Tight-Binding Simulation

Gerhard Klimeck^{a*}, Chris Bowen^a, and Timothy B. Boykin^b

^a Jet Propulsion Laboratory, California Institute of Techn., Pasadena, CA 91109

^b The University of Alabama in Huntsville, Huntsville, AL 35899

Abstract. Heterointerfaces, applied bias and built-in potentials break the symmetry of the crystalline lattice in a resonant tunneling diode (RTD) which causes a strong interaction of heavy-, light- and split-off hole bands. This interaction leads to hole transport paths which are significantly more complicated than the paths for electrons. Compared to a direct bandgap electron RTD where most of the carriers are transported straight through the structure (zero transverse momentum) it is shown here that in the hole case most of the holes are transported through the structure at an angle (non-zero transverse momentum) for a wide range of bias points.

1. Introduction

Atomistic Modeling is needed to treat material variations on an atomic scale that enable the quantum mechanical functionality of devices such as resonant tunneling diodes (RTDs). To enable the exploration of the vast heterostructure design space a general purpose quantum mechanics-based 1-D device design and analysis tool entitled NEMO (Nanoelectronic Modeling) has been developed [1]. NEMO is based [2] on the non-equilibrium Green function approach, which allows a fundamentally sound inclusion of the required physics: bandstructure, scattering, and charge self-consistency and it has shown [3,4] to have predictive simulation capabilities. More information on NEMO, including how to obtain a copy of the software, can be found on web sites [1].

Hole Transport Analysis for Optical Devices: Quantum mechanical carrier transport research has focused on pure electron transport since most high speed quantum devices utilize the high electron mobility in III-V materials. However, typical optical devices also involve quantum states in the valence bands. Interband quantum cascade lasers in particular involve direct tunneling between conduction and valence bands. To begin a NEMO study of quantum mechanical carrier transport in such structures the coherent transport in a simple hole-doped RTD is examined.

Previous Research has shown [5–8] that hole transport is strongly influenced by coupling between the light hole (LH), heavy hole (HH) and split-off (SO) valence bands. The valence bands are coupled intrinsically by the spin-orbit interaction and by translational symmetry breaking induced by material variations and internal or external fields. Envelope function representations have been used extensively in much of the published work on hole transport [9–15]. This paper is an extension of previous work by Kiledjian et.al. [16] who use a nearest-neighbor sp^3s^* empirical tight-binding basis which includes the spin-orbit interaction to all orders and incorporates wavefunction coupling at interfaces through orbital interactions. We include both nearest and 2nd-nearest neighbor interactions [17] to better fit the

complicated valence band dispersion.

Parallelization of the NEMO code on various simultaneous levels (voltage, transverse momentum integration and energy integration) and the use of massively parallel computers enabled the thorough exploration of the state space in total energy E and transverse momentum k for a significant number of bias points. The main point of this paper is to contrast qualitative differences between electron and hole transport in RTD's. The resolution of the transverse momentum k of the carriers will be used visualize the qualitative differences.

2. Momentum dependent Current Density $J(k)$

If incoherent scattering in the central device region can be ignored the current can be computed [2,3] using an expression of the form:

$$J \propto \int dE \int k dk T(E, k) (f_L(E) - f_R(E)) = \int dE \int k dk J(E, k) \quad (1)$$

$$= \int k dk J(k) \quad \text{with : } J(k) = \int dE J(E, k) \quad (2)$$

where k is the electron momentum transverse to the transport direction normalized to the unit cell a by $\frac{\pi}{a}$, E is the total energy, T the transmission coefficient, and $f_{L/R}$ the Fermi function in the left/right contact. The dependence of the transmission coefficient on the momentum angle ϕ has been found [18] to be weak in the material and device system studied here. To gain insight as to “where” the carriers flow with respect to the transverse momentum quantum number we define the intermediate quantity $J(k)$.

3. Tsu-Esaki Formula

One common approach in reducing the required CPU time needed to compute a complete I-V characteristic is the assumption of parabolic transverse subbands such that the transmission coefficient has a analytic, parabolic transverse momentum dependence: $T(E, k) = T(E - \hbar^2 k^2 / 2m^*, k=0)$. Under this assumption the transverse momentum integration in Eq. 1 can be carried out analytically to result in the so-called Tsu-Esaki [19] formula:

$$J \propto \rho_{2D} \int dE T(E, k=0) \ln \left(\frac{1 + e^{(E_F - E)/kT}}{1 + e^{(E_F - E - qV)/kT}} \right) \quad (3)$$

This paper will show in the next section an example of good [20] agreement between the Tsu-Esaki approximation and the full numerical integration for a structure that has flat band conditions in the emitter and therefore provides a 3-D emitter to 2-D quantum well tunneling process. We emphasize here in advance that such a simulation is included for paedagogical reasons, to show the simple behavior of $J(k)$ for electrons. The rest of the paper underlines that the analytical Tsu-Esaki integration becomes completely invalid for hole transport [16].

4. The Model Structures

To simplify the analysis of the hole transport case we consider the most trivial RTD structure of flat emitter and collector bands and a linear potential drop along the barriers and well. The barriers

and well are 10 and 20 monolayers thick, respectively. The emitter, collector and well are taken to be GaAs. The hole/electron RTD is assumed to have AlAs / $\text{Al}_{0.4}\text{Ga}_{0.6}\text{As}$ barriers [21]. The doping in the contacts is set to 10^{18} cm^{-3} . The second nearest neighbor sp³s* tight binding parameters for these three materials can be found in [18].

5. Monotonic Momentum Dependence of RTD Electron Transport

Figure 1a) shows the familiar transmission coefficient through an electron RTD at zero transverse momentum. Figure 1b) shows the expected transverse dispersion for the ground and first excited state in a GaAs/AlGaAs RTD. Some non-parabolicity is evident in the first excited state (decreasing state separation with increasing k). Figure 1c) shows the transmission coefficient for a non-zero transverse momentum. This transmission coefficient appears qualitatively to be just energy shifted from the one in Figure 1a) disregarding non-parabolicity in the second state and the non-unity transmission resonance. That is exactly the assumption that enters into the derivation of the Tsu-Esaki formula (Eq. 3).

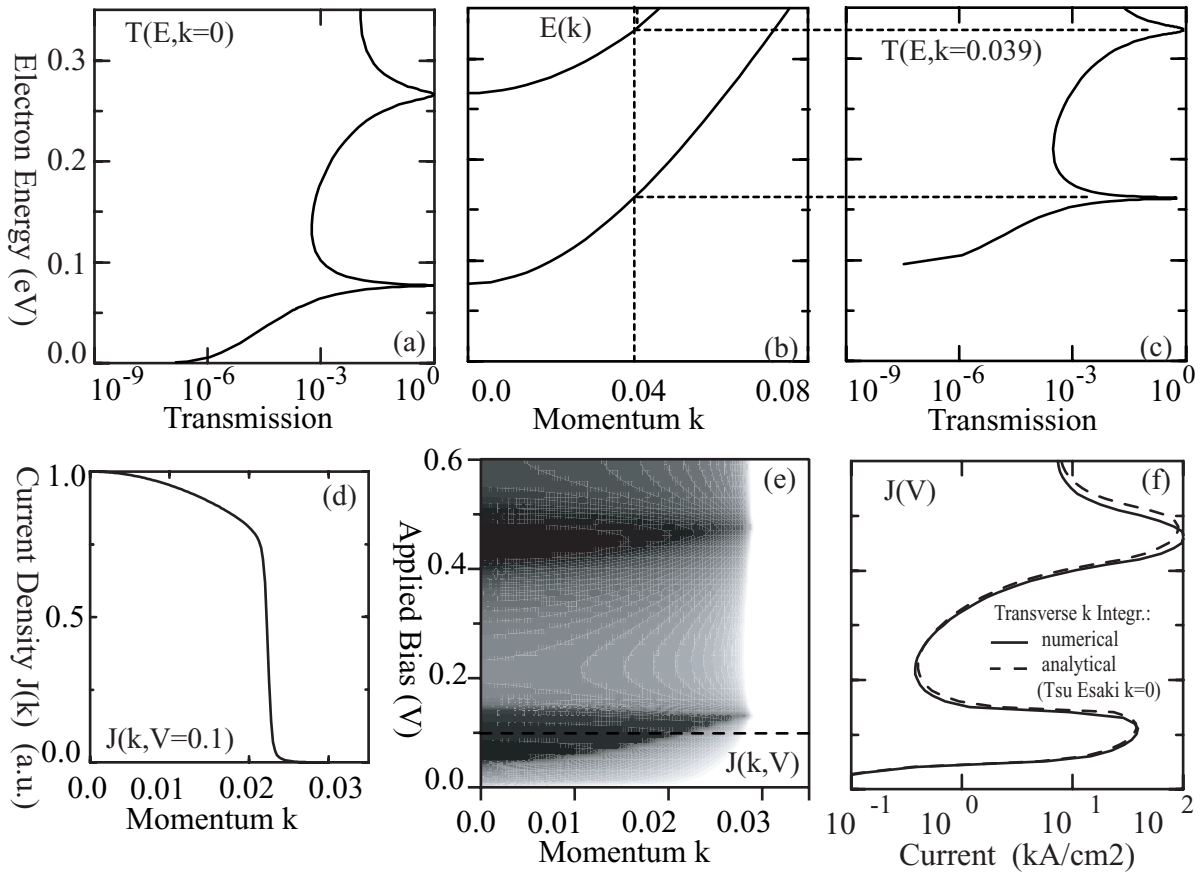


FIG. 1. Transport in an electron RTD. (a) Transmission coefficient $T(E, k = 0)$. (b) Transverse electron subband. (c) Transmission coefficient $T(E, k = 0.039)$. Curve is qualitatively identical to (a) except for the shift in energy. (d) Current density $J(k, V = 0.1 \text{ V})$ as a function of momentum k at a bias of 0.1V. $J(k, V = \text{const})$ is monotonically decreasing. (e) Current density $J(k, V)$ as a function of transverse momentum k and applied Voltage V on a logarithmic gray contour scale (dark=high, light=low). Dark regions indicate the emitter Fermi sea passing through the resonances. $J(k, V = \text{const})$ is monotonically decreasing for all k . Dashed horizontal line references the cut along $V = 0.1 \text{ V}$ in (d). (f) Current voltage characteristic $J(V)$ after integration over transverse momentum.

In Figure 1e) the current density spectrum of $J(k, V)$ is shown as a function of transverse momentum k and applied voltage V on a logarithmic contour gray scale plot. Dark/light shades indicate high/low density, respectively. The dark filled parabolic region corresponding to the parabolic dispersion of the ground state is a nice depiction of the Fermi sea of electrons that is allowed to flow through a structure where the emitter and quantum well dispersion are identical.

Figure 1d) shows a cut through Figure 1e) along the momentum axis k for a constant bias of $0.1V$. $J(k)$ is simply monotonically decreasing. It can be shown analytically [18] for electrons that are injected from a 3-D emitter with the same effective mass as the RTD well that $J(k)$ is monotonically decreasing with transverse momentum k independent of the applied bias. The following section will contrast the differences of electron and hole transport with respect to the behavior of $J(k)$.

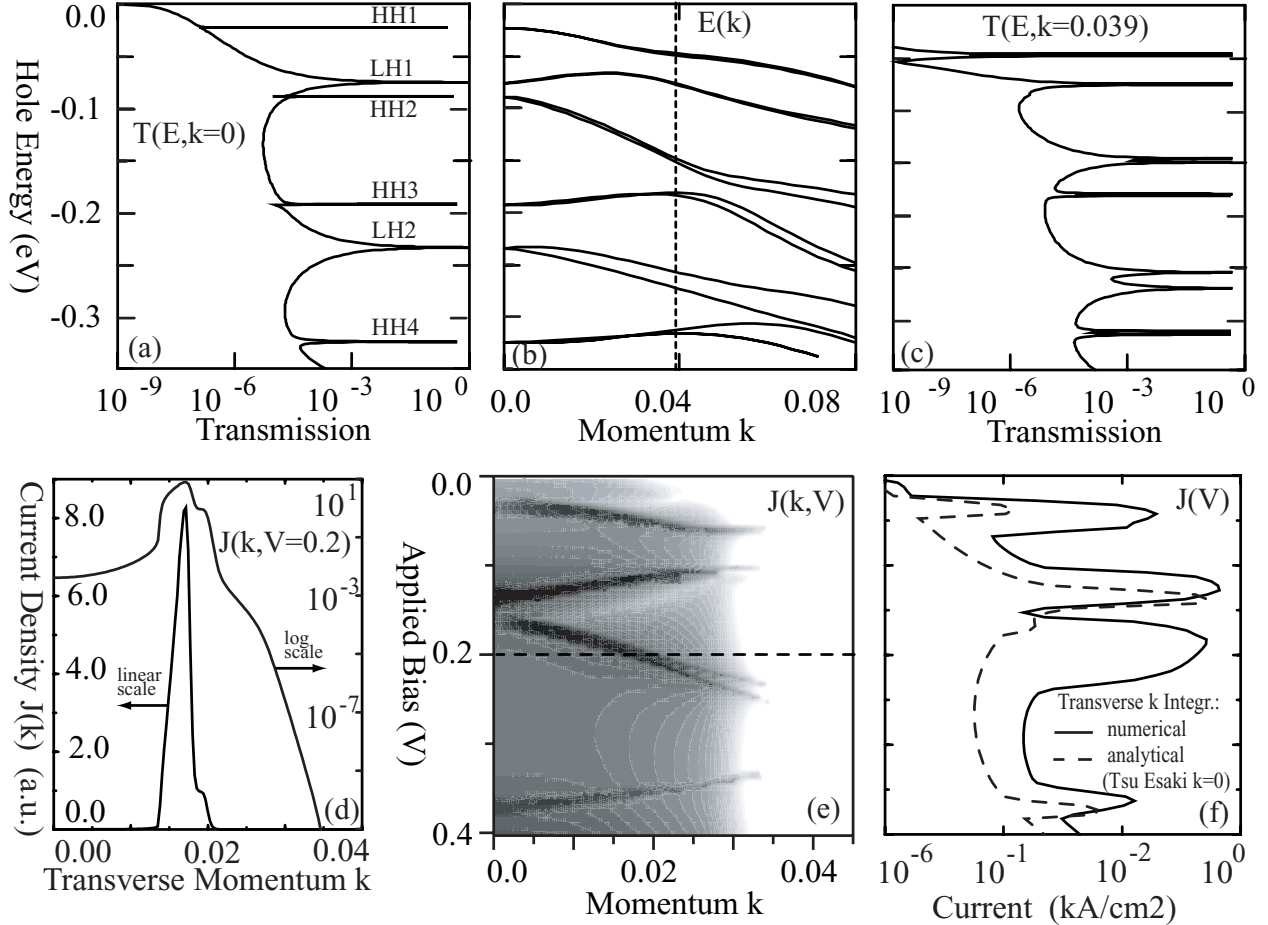


FIG. 2. (a) Transmission coefficient $T(E, k = 0)$. (b) Transverse hole subband. (c) Transmission coefficient $T(E, k = 0.039)$. The transmission coefficient in (c) is clearly not just an energy shifted version of the transmission coefficient of (a). (d) Current density $J(k, V = 0.2V)$ as a function of momentum k at a bias of $0.2V$. $J(k, V = \text{const})$ shows sharp spectral features as a function of momentum k on a linear as well as a logarithmic scale. (e) Current density $J(k, V)$ as a function of transverse momentum k and applied Voltage V on a logarithmic gray contour scale (dark=high, light=low). Dark streaks indicate narrow regions of high current density in the (k, V) space. Dashed horizontal line references the cut along $V = 0.2V$ in (d). (f) Current voltage characteristic $J(V)$ after integration over transverse momentum. The analytical (Tsu-Esaki) integration misses several current channels that are open for $k \neq 0$.

Figure 1f) shows two current voltage characteristics computed in the electron case with numerical and analytical transverse momentum integration. Since we considered a 3-D emitter and a material system with little non-parabolicity we observe a good agreement [20] between the two computational results.

6. Spiked Momentum Dependence of RTD Hole Transport

Figure 2 is in its structure similar to Figure 1. The top panel (2a-c)) shows the transmission coefficients and $E(k)$ dispersion at zero bias for the hole RTD. Note that the dispersion in Figure 2b) is anything but parabolic. The various heavy hole (HH) and light hole (LH) resonance states are strongly interacting as evident by the various anti-crossings. The interaction creates strong variations in the transmission coefficients as a function of transverse momentum.

As the strongly k -dependent transmission coefficients are integrated over total energy E one expects to see strong variations in $J(k)$ with the transverse momentum k . This is indeed displayed in Figure 2e) where $J(k, V)$ is plotted as a function of transverse momentum k and applied voltage V on a logarithmic contour gray scale plot. Dark/light shades indicate high/low density, respectively. Unlike the electron picture of Figure 1e) we now see distinct streaks of high current density in the (k, V) space. Interestingly these streaks follow the hole dispersion in Figure 2b) closely to the emitter Fermi wavevector at about $k_F \approx 0.029$. Indeed a close connection between the two spectra can be established analytically [18]. These streaks of current develop since the (almost) parabolic dispersion in the emitter and the highly non-parabolic dispersion in the well create non-trivial transverse momentum conserving selection rules [18].

Figure 2d) shows a cut through Figure 2e) along the momentum axis k for a constant bias $0.2V$. Sharp spectral features as a function of transverse momentum k on a linear as well as a logarithmic scale are visible. Figure 2d) shows that most of the carriers are flowing through the structure with a non-zero transverse momentum. Since the high current density streaks in Figure 2e) move along a wide bias range it is clear that the hole transport is off-zone center for a wide bias range.

The current voltages shown in Figure 2f) show that the analytical transverse momentum integration completely misses some of the conduction channels. The Tsu-Esaki approximation breaks down completely and a full numerical transverse momentum integration is therefore necessary to capture all the conduction channels.

6. Summary and Conclusions

This work demonstrates the qualitatively different carrier spectra in hole and electron transport through very simple structures. It has been shown that the majority of holes travels through the structure at an angle (with non-zero transverse momentum) rather than straight through for a large range of bias points.

To achieve a numerically noiseless current voltage characteristic in the hole RTD we included about 140 numerical k points in the range of $[0...0.045]$ on a uniform k -grid. Such computations require about 3 days of computing time on a 32 CPU beowulf cluster consisting of Intel Pentium III processors running at 450MHz. Since our past experience with electron transport has been that $J(k)$ varies smoothly and a homeogeneous k -grid with only few k points provided excellent results we had not incorporated an adaptive k -grid. To optimize the computational performance one could introduce an adaptive k -grid integration similar to the the adaptive energy grid integration we are performing

already.

With the insight of “where” the carriers flow in momentum and energy space we can now proceed to simulate experimental hole RTDs and study interband transport occurring in Sb-based RTDs and cascade lasers.

7. Acknowledgements

The research described in this paper was carried out at the Jet Propulsion Laboratory, California Institute of Technology, under a contract with the National Aeronautics and Space Administration. The supercomputers used in this investigation were provided by funding from the NASA Offices of Earth Science, Aeronautics and Space Science.

References

- * Correspondence email: gekco@jpl.nasa.gov On the web: <http://hpc.jpl.nasa.gov/PEP/gekco>
- [1] See <http://hpc.jpl.nasa.gov/PEP/gekco/nemo> or search for NEMO on <http://www.raytheon.com>.
- [2] R. Lake, G. Klimeck, R. C. Bowen, and D. Jovanovic, J. Appl. Phys. **81**, 7845 (1997).
- [3] R. C. Bowen *et al.*, J. Appl. Phys. **81**, 3207 (1997).
- [4] G. Klimeck *et al.* in the *1997 55th Annual Device Research Conference Digest*, (IEEE, NJ, 1997), p. 92.
- [5] E. E. Mendez, W. I. Wang, B. Ricco, and L. Esaki, Applied Physics Letters **47**, 415 (1985).
- [6] R. K. Hayden *et al.*, Physical Review Letters **66**, 1749 (1991).
- [7] J. A. Kash, M. Zachau, M. A. Tischler, and U. Ekenberg, Physical Review Letters **69**, 2260 (1992).
- [8] W.-C. Tan, J. C. Inkson, and G. P. Srivastava, Physical Review B **54**, 14623 (1996).
- [9] J. M. Luttinger and W. Kohn, Physical Review **97**, 869 (1955).
- [10] M. Burt, Semicond. Sci. Technol. **3**, 739 (1988).
- [11] B. Foreman, Physical Review Letters **81**, 425 (1998).
- [12] S. Ekbote, M. Cahay, and K. Roenker, Phys. Rev. B **58**, 16315 (1998) and J. of Appl. Phys. **87**, 1467(2000).
- [13] C. Y.-P. Chao and S. L. Chuang, Physical Review B **43**, 7027 (1991).
- [14] Y. X. Liu, R. R. Marquardt, D. Z.-Y. Ting, and T. C. McGill, Physical Review B **55**, 7073 (1991).
- [15] J. X. Zhu, Z. D. Wang, and C. D. Gong, Solid State Communications **101**, 257 (1997).
- [16] M. S. Kiledjian, J. N. Schulman, K. L. Wang and K. V. Rousseau, Phys. Rev. B, **46**, 16012 (1992) and Surface Science **267**, 405 (1992).
- [17] T. Boykin, L. J. Gamble, G. Klimeck, and R. C. Bowen, Physical Review B **59**, 7301 (1999).
- [18] Gerhard Klimeck, R. Chris Bowen and Timothy B. Boykin, submitted to Phys. Rev. B (2000).
- [19] R. Tsu and L. Esaki, Appl. Phys. Lett. **22**, 562 (1973).
- [20] The Tsu-Esaki 1-D integration formula is capable of providing qualitatively correct results for electron devices given the restrictive assumption that subband alignment is *not* the primary transport mechanism [3,22–24]. Technologically relevant RTDs that show negative differential resistance at room temperature all exhibit a triangular emitter well such that there is a large 2-D to 2-D subband tunneling contribution from emitter to central resonance. To achieve quantitative agreement [3,4] between simulation and experimental data for such RTDs full 2-D integrations in energy E and transverse momentum k must be performed.
- [21] Using $\text{Al}_{0.4}\text{Ga}_{0.6}\text{As}$ instead of AlAs barriers for the electron RTD avoids any additional complications due to confined X states in the barriers.
- [22] T. B. Boykin, R. E. Carnahan, and R. J. Higgins, Phys. Rev. B **48**, 14232 (1993).
- [23] T. B. Boykin, R. E. Carnahan, and K. P. Martin, Phys. Rev. B **51**, 2273 (1995).
- [24] T. B. Boykin, Phys. Rev. B **51**, 4289 (1995).